Role of a Guanidinium Cation−Phosphodianion Pair in Stabilizing the Vinyl Carbanion Intermediate of Orotidine 5′-Phosphate Decarboxylase-Catalyzed Reactions

Bogdana Goryanova,[†] Lawrence M. Goldman,[†] Tina L. Amyes,[†] John A. Gerlt,[‡] and John P. Richard*[,†]

[†]Department of Chemistry, University at Buffalo, Buffalo, New York 14260, United States
[‡]Department of Biochemistry and Chemistry, University of Illinois, Urbana, Illinois 61801, United States

S *Supporting Information*

ABSTRACT: The side chain cation of Arg235 provides a 5.6 and 2.6 kcal/mol stabilization of the transition states for orotidine 5′-monophosphate (**OMP**) decarboxylase (OMPDC) from *Saccharomyces cerevisiae* catalyzed reactions of **OMP** and 5-fluoroorotidine 5′-monophosphate (**FOMP**), respectively, a 7.2 kcal/mol stabilization of the vinyl carbanion-like transition state for enzyme-catalyzed exchange of the C-6 proton of 5-fluorouridine 5′-monophosphate (**FUMP**), but no stabilization of the transition states for enzyme-catalyzed decarboxylation of truncated substrates 1-(β-D-erythrofuranosyl)orotic acid and 1-(β-D-erythrofuranosyl) 5-fluorouracil. These observations show that the transition state stabilization results from formation of a protein cation−phosphodianion pair, and that there is no detectable stabilization from an interaction between the side chain and the pyrimidine ring of substrate. The 5.6 kcal/mol side chain interaction with the transition state for the decarboxylation reaction is 50% of the total 11.2 kcal/mol transition state stabilization by interactions with the phosphodianion of **OMP**, whereas the 7.2 kcal/mol side chain interaction with the transition state for the deuterium exchange reaction is a larger 78% of the total 9.2 kcal/mol transition state stabilization by interactions with the phosphodianion of **FUMP**. The effect of the R235A mutation on the enzyme-catalyzed deuterium exchange is expressed predominantly as a change in the turnover number k_{ex}, whereas the effect on the enzyme-catalyzed decarboxylation of **OMP** is expressed predominantly as a change in the Michaelis constant K_m. These results are rationalized by a mechanism in which the binding of **OMP**, compared with that for **FUMP**, provides a larger driving force for conversion of OMPDC from an inactive open conformation to a productive, active, closed conformation.
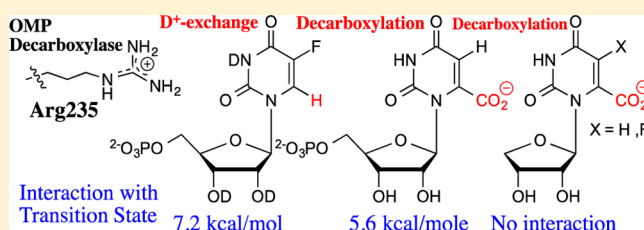
The mechanism of action of orotidine 5′-monophosphate decarboxylase (OMPDC) has attracted the interest of enzymologists and other chemists interested in catalysis because of the difficulty in rationalizing the enormous 10^{17}-fold enzymatic rate acceleration of chemically difficult non-enzymatic decarboxylation of orotidine 5′-monophosphate (**OMP**, Scheme 1A, X = H) to give uridine 5′-monophosphate (**UMP**).[1,2] The well-known large barrier to nonenzymatic decarboxylation of OMP, which arises from the great instability of the putative vinyl carbanion reaction intermediate,[3–5] prompted proposals of reaction mechanisms that avoid formation of this intermediate[6–12] but surprisingly, little experimental data in support of any mechanism, until it was shown that OMPDC catalyzes both the decarboxylation of **OMP** and 5-fluoroorotidine 5′-monophosphate (**FOMP**, Scheme 1A, X = F) and exchange of the C-6 proton of **UMP** and of 5-fluorouridine 5′-monophosphate (**FUMP**) for deuterium from solvent D$_2$O (Scheme 1B).[13–15] These results provide compelling evidence that OMPDC-catalyzed reactions are through a vinyl carbanion reaction intermediate that is strongly stabilized by interactions with the protein catalyst. The unusual failure of OMPDC to differentiate between the reaction of hydrogen and deuterium, from a mixed solvent of 50/50 H$_2$O/D$_2$O, in protonation of the vinyl carbanion is consistent with a short lifetime for the reaction intermediate.[16,17]

OMPDC provides a large ∼31 kcal/mol stabilization of the transition state for the decarboxylation of OMP and a smaller ∼8 kcal/mol stabilization of the Michaelis complex.[1] These observations show that it is necessary to determine both the network of stabilizing protein−transition state interactions and the mechanism by which these interactions develop on moving from the Michaelis complex to the reaction transition state. The interactions between OMPDC and the substrate phosphodianion provide an 11.2 kcal/mol stabilization of the transition state for decarboxylation, which is 40% of the total transition state stabilization.[18,19] Interactions between OMPDC and the phosphodianion of 5-fluorouridine 5′-monophosphate (FUMP) provide a smaller 9.2 kcal/mol stabilization of the transition state for the enzyme-catalyzed deuterium exchange reaction.[20] This intrinsic phosphodianion binding energy is
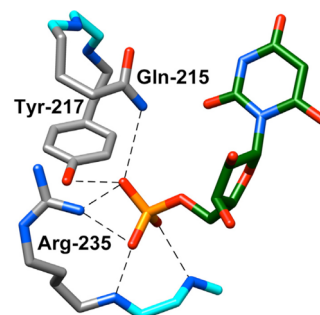
Scheme 1
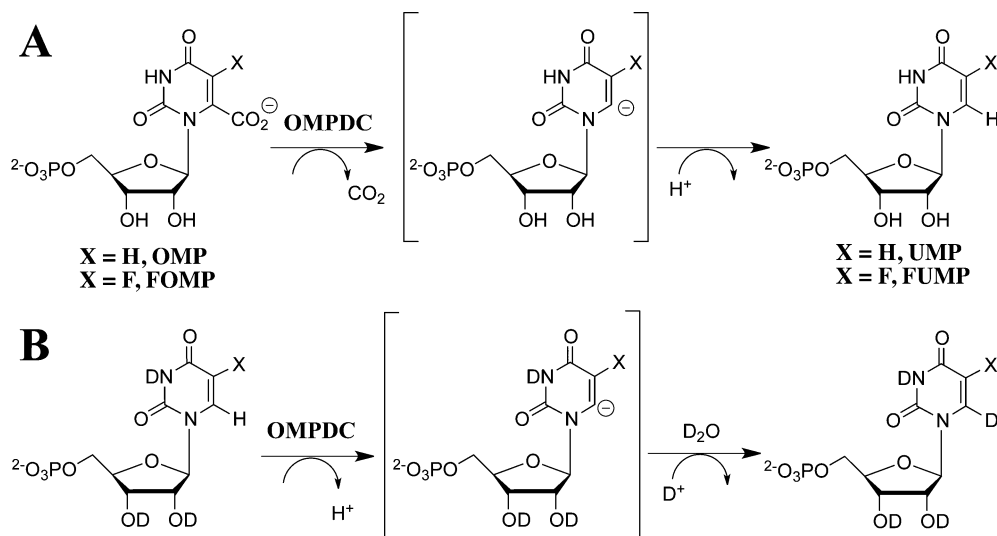
similar to that determined for the proton and hydride-ion transfer reactions, catalyzed by triosephosphate isomerase and α-glycerol phosphate dehydrogenase, respectively.[21–24]

The 9−11 kcal/mol phosphodianion binding energy might be utilized to anchor the substrate to OMPDC (K_m effect) or to activate the enzyme for catalysis of the decarboxylation and deuterium exchange reactions in which case the binding interactions will be expressed specifically at the transition state for the enzyme-catalyzed reaction (k_{cat} effect).[25] We have distinguished between anchoring and activating interactions of OMPDC with the phosphodianion of **OMP** or **FUMP** by cutting the covalent connection that anchors the phosphodianion to the whole substrates and examining the OMPDC-catalyzed reactions of substrate pieces (Scheme 2). The binding of the phosphite dianion (HPO_3^{2-}) to OMPDC results in a large increase in the observed second-order rate constant k_{cat}/K_m for enzyme-catalyzed decarboxylation of 1-(β-D-erythrofuranosyl)orotic acid (**EO**) and the deuterium exchange

reaction of 1-(β-D-erythrofuranosyl)-5-fluorouracil (**FEU**) (Scheme 2).[18,20] This is the result of utilization of protein−dianion binding interactions to activate OMPDC for catalysis of reactions at the distant pyrimidine ring.

The X-ray crystal structure of OMPDC from *Saccharomyces cerevisiae* (*Sc*OMPDC) liganded with 6-hydroxyuridine 5′-monophosphate (Figure 1) shows that the phosphodianion
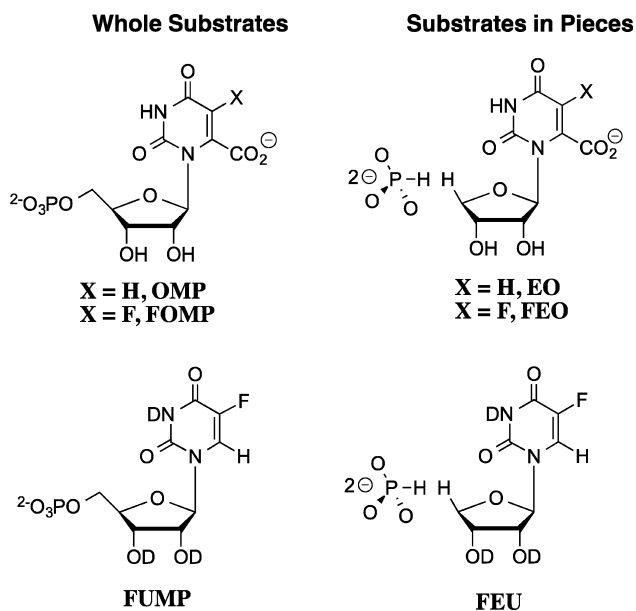

Figure 1. X-ray crystal structure of yeast OMPDC liganded with 6-hydroxyuridine 5′-monophosphate (Protein Data Bank entry 1DQX).[2] The structure shows the interactions between the side chains of Gln215, Tyr217, and Arg235 of the protein with the bound phosphodianion group. Reprinted with permission from ref 19. Copyright 2012, American Chemical Society.

group of the ligand interacts directly with the side chains of Gln215 and Tyr217, which are part of a closed flexible loop, and with the guanidinium group of Arg235.[2] The focus of this paper is the strong ion-pairing interaction between the phosphodianion and the guanidinium cation side chain of Arg235 that accounts for 50% of the total intrinsic phosphodianion binding energy.[26,27] We are interested in determining whether these interactions are expressed at the transition state for the OMPDC-catalyzed deuterium exchange reaction of **FUMP**, in which case they would be utilized mainly in the stabilization of the vinyl carbanion intermediate common to the decarboxylation and deuterium exchange reactions.

We report the effect of the R235A mutation of *Sc*OMPDC on the kinetic parameters for the following enzymatic reactions: (1) the enzyme-catalyzed deuterium exchange reaction of **FUMP**, (2) the rescue, by guanidinium cation, of the activity of

Scheme 2

the R235A mutant of OMPDC for catalysis of the deuterium exchange reaction of **FUMP**, and (3) the enzyme-catalyzed decarboxylation of **FOMP** and of the truncated substrate 1-(β-D-erythrofuranosyl) 5-fluoroorotic acid (**FEO**). These data are analyzed along with results from earlier studies of the effect of the R235A mutation on OMPDC-catalyzed decarboxylation of **OMP** and **EO**.[19,28]

■ EXPERIMENTAL SECTION

Materials. D-Ribose 5-phosphate (disodium salt ≥98%), 5-fluorouridine (99%), phosphoryl chloride (99%), phosphoenolpyruvate (monosodium salt, 98%), adenosine 5′-triphosphate (disodium salt, 99%), β-nicotinamide adenine dinucleotide (disodium salt, 98%), and triethylamine (99.5%) were purchased from Sigma. 3-(N-Morpholino)propanesulfonic acid (99.5%) and trimethyl phosphate (97%) were purchased from Fluka, imidazole (99.5%), guanidinium hydrochloride (99%), and potassium phosphate (99.8%) were from Fisher. Ultrapure glycylglycine (>99%) was obtained from USB Biochemicals. Dowex-50 (hydrogen form), DEAE Sephadex A-25, and Amberlite IR120 ion exchange resins were purchased from Sigma. The following deuterium labeled compounds were purchased from Cambridge Isotope Laboratories: D_2O (99.9%), DCl (35 wt %, 99.9% D), and NaOD (30 wt %, 98% D). The water was distilled and purified in a Milli-Q water purification system. The imidazole was recrystallized from benzene and dried under vacuum at room temperature for several days. Trimethyl phosphate was dried over activated molecular sieves (4 Å) and distilled under reduced pressure. 5-Fluorouridine was dried at 50 °C under reduced pressure for 24 h prior to use. All other reagents were used without further purification.

L-Lactate dehydrogenase, inorganic pyrophosphatase, adenylate kinase, and pyruvate kinase were purchased from Sigma. Orotate phosphoribosyl transferase (ORTase) from *Salmonella typhimurium* was overexpressed in *Escherichia coli* BL21 (DE3) transformed with the plasmid pOPRTase.[29] The isolated OPRTase was purified according to a literature procedure.[30] Phosphoribosylpyrophosphate (PRPP) synthetase from *E. coli* was constitutively expressed from *E. coli* strain HO1702 harboring the plasmid pHO11 that was a generous gift from Professor Vern Schramm[31,32] and was purified according to a literature procedure.[33] Published procedures were followed to prepare wild-type OMPDC from *Saccharomyces cerevisiae* (*Sc*OMPDC) and the R235A mutant of *Sc*OMPDC.[27]

Orotidine 5′-monophosphate was prepared by enzymatic methods from orotate and phosphoribosylpyrophosphate.[34] This synthesis gave **OMP** that contained ammonium bicarbonate from purification by column chromatography that was removed by the following procedure. Stock solutions of **OMP** (~10−25 mM) were carefully titrated to pH 5 with 1.00 M HCl, and N_2 was then bubbled through the solution to carry away CO_2. The solution pH was adjusted to 7.1 and monitored for several hours. If an increase in pH was observed due to the evaporation of CO_2, then additional 1.00 M HCl was added and the bubbling of nitrogen repeated. The concentration of NH_4Cl in the final NH_4CO_3 free solution was determined as the concentration of HCl used to convert the HCO_3^- to CO_2. The concentration of this salt was included in the calculation of the solution ionic strength.

The triethylammonium salt of **FUMP** was synthesized as described in earlier work[13] and was converted to the free acid by passage over Amberlite IR120 resin (H^+-form) in methanol.

1-(β-D-Erythrofuranosyl) 5-fluoroorotic acid (**FEO**) was synthesized as described in earlier work.[28] 5-Fluoroorotidine 5′-monophosphate (**FOMP**) was synthesized enzymatically by adaptation of the procedure for the enzymatic synthesis of **UMP**.[35] A typical reaction mixture (10 mL, 30 °C) contained, initially, 0.25 mmol of 5-fluoroorotic acid, 4 units of PRPP synthase, 20 units of ORTase, 200 units of adenylate kinase, 200 units of pyruvate kinase, 300 units of yeast inorganic pyrophosphatase, 50 mM $MgCl_2$, 3 mM ATP, 60 mM PEP, and 3 mM DTT in 30 mM phosphate buffer at pH 7.5. The formation of **FOMP** was monitored in aliquots that were diluted 250-fold into an assay mixture for OMPDC by determining the decrease in absorbance at 282 nm from OMPDC-catalyzed decarboxylation of **FOMP**. The yield of **FOMP** plateaued after 90 min, at which time an additional 0.25 mmol of 5-fluoroorotic acid was added. The reaction was monitored for an additional 150 min, when the yield of **FOMP** again plateaued. The enzymes were removed by filtration using an Amicon Ultra-15 10 KDa MWCO membrane centrifugal filter, and the **FOMP** was purified by ion exchange chromatography over DEAE Sephadex A25 and eluting with a gradient of triethylammonium bicarbonate. The fractions that contained **FOMP** were pooled, and the buffer salts were removed on a rotary evaporator at reduced pressure followed by lyophilization. The lyophilizate was suspended in 25 mL of methanol that contained 25 g of Amberlite IR120 resin (H^+ form). The solution was stirred for 1 h at room temperature with gentle purging of Ar. The resin was then removed by filtration, washed with 200 mL of methanol, and the solvent was removed under reduced pressure. The compound was dissolved in water, and colored material from the Amberlite resin was removed by passage through a 3 mL Supelco reversed phase (LC-18) SEP tube. This gave the free acid of **FOMP** as a colorless solid in 40% yield.

NMR Analyses. ^{19}F NMR spectra were acquired on a Varian Unity Inova-500 spectrometer operating at 470 MHz. Spectra (64 transients), obtained to monitor enzyme-catalyzed deuterium exchange reactions, were recorded using a spectral width of 50 000 Hz, a 90° pulse angle, a 2.6 s acquisition time, and a relaxation delay between pulses of 28 s ($>7T_1$).[20] The chemical shifts of the ^{19}F NMR signals are referenced to the value of −78.5 ppm for a neat trifluoroacetic acid external standard.

Preparation of Solutions. The solution pH was determined at 25 °C using an Orion Model 720A pH meter equipped with a Radiometer pHC4006-9 combination electrode that was standardized at pH 7.00 and 10.00 at 25 °C. The pD of the buffers prepared in D_2O was obtained by adding 0.4 to the reading on the pH meter.[36] The acidic protons of GlyGly were exchanged for deuterium by dissolving the buffer in D_2O followed by evaporation and drying under vacuum at 55 °C. Buffered solutions of GlyGly were prepared by dissolving the buffer acid in D_2O and adjusting to the required pD using 0.98 M NaOD. The concentration of **FOMP** and **FUMP** in 0.1 M HCl was determined from the absorbance at 271 nm ($\varepsilon = 10200$ M^{-1} cm^{-1}) and 270 nm ($\varepsilon = 9160$ M^{-1} cm^{-1}), respectively.[13,28] Samples of R235A mutant *Sc*OMPDC that had been stored at −80 °C were defrosted and dialyzed at 7 °C against 50 mM MOPS (45% free base) at pH 7.0 and $I = 0.14$ (NaCl) for the experiments with **FEO**. Samples of wild-type *Sc*OMPDC were dialyzed at 7 °C against 10 mM MOPS at pH 7.1 and $I = 0.10$ (NaCl). Samples of R235A mutant *Sc*OMPDC used to study catalysis of the deuterium exchange

reaction were dialyzed at 7 °C against 10 mM MOPS at pH 7.1 and $I = 0.10$ (NaCl). This was followed by dialysis against several changes of 60 mM GlyGly (pD 8.15) at $I = 0.14$ (NaCl) in D_2O using a D-tube dialyzer (10 kDa MWCO, Novagen) placed inside a narrow vessel that was isolated from atmospheric moisture using parafilm. The concentration of stock solutions of wild-type R235A mutant ScOMPDC was determined from the absorbance at 280 nm by using an extinction coefficient of 29 900 M^{-1} cm^{-1}, calculated with the ProtParam tool available on the ExPASy server.[37]

Steady-State Enzyme Kinetics. The decarboxylation of OMP catalyzed by OMPDC was monitored spectrophotometrically by following the decrease in absorbance at 279, 290, or 295 nm [$\Delta\varepsilon$, λ: −2400 M cm^{-1}, 279 nm; −1620 M cm^{-1} 290 nm; −842 M cm^{-1}, 295 nm]. These wavelengths were chosen so that the initial absorbance A_i were ≤2.0. Assays (1 mL) contained **OMP** (0.05−1.5 mM) at pH 7.1 (30 mM MOPS), 25 °C, and at $I = 0.10$ maintained with NaCl. The reactions were initiated by the addition of a stock solution of R235A mutant ScOMPDC to give a final enzyme concentration of 1 μM. The initial velocity v_i (M s^{-1}) was determined by monitoring the decrease in absorbance at the chosen wavelength. Values of k_{cat} and K_m were obtained from the nonlinear least-squares fits of seven or more values of $v_i/[E]$ (s^{-1}) to the Michaelis−Menten equation.

Assays of R235A mutant ScOMPDC-catalyzed decarboxylation of **FOMP** contained **FOMP** (0.10−1.0 mM) at pH 7.1 (10 mM MOPS), 25 °C, and $I = 0.10$ maintained with NaCl. Initial velocities, v_i (M s^{-1}), of the decarboxylation of **FOMP** catalyzed by R235A mutant ScOMPDC were determined spectrophotometrically by monitoring the decrease in absorbance at 290 nm ($\Delta\varepsilon = -1090$ M^{-1} cm^{-1}). Assays in a volume of 1 mL were initiated by the addition of 1 μL of a stock solution of R235A mutant ScOMPDC to give a final enzyme concentration of 15−20 nM. Values of k_{cat} and K_m for the R235A ScOMPDC-catalyzed decarboxylation reaction of **FOMP** were obtained from the nonlinear least-squares fit of the values of $v_i/[E]$ to the Michaelis−Menten equation.

R235A ScOMPDC-Catalyzed Decarboxylation of FEO. The decarboxylation of **FEO** (0.14 mM) catalyzed by R235A mutant ScOMPDC (30 μM) at pH 7.0 (25 mM MOPS), 25 °C, and an ionic strength of 0.14 (NaCl) was followed spectrophotometrically by monitoring the decrease in absorbance at 282 nm, as described in a previous study using wild-type ScOMPDC.[28] These reactions were monitored for ≥10 reaction half-times (≤800 min), during which time ScOMPDC was shown by a standard enzyme assay to maintain full catalytic activity. Observed first-order rate constants k_{obs} (s^{-1}) for enzyme-catalyzed decarboxylation of **FEO** were obtained from the fits of reaction progress curves to an equation for a single exponential decay.[18] Second-order rate constants (k_{cat}/K_m)$_{obs}$ were obtained using the relationship (k_{cat}/K_m)$_{obs}$ = $k_{obs}/[E]$.

R235A ScOMPDC-Catalyzed Deuterium Exchange at C-6 of h-FUMP Monitored by ^{19}F NMR Spectroscopy. The C-6 deuterium exchange reactions of h-FUMP catalyzed by the R235A mutant of ScOMPDC in D_2O at pD 8.15 were monitored by ^{19}F NMR spectroscopy at 470 MHz. Reactions in a volume of 1−2 mL were initiated by the addition of an aliquot of h-FUMP in D_2O to a mixture of 50 mM GlyGly (20% free base) at pD 8.15, NaCl, and the R235A mutant of ScOMPDC in D_2O to give final concentrations of 0.74−9.6 mM h-FUMP and of 0.2−0.9 mM mutant ScOMPDC at $I = 0.14$. In experiments where the effect of guanidinium cation on the

velocity of the enzyme-catalyzed deuterium exchange reaction was examined, reactions in a volume of 1−2 mL were initiated by addition of an aliquot of h-FUMP in D_2O to a mixture of 50 mM GlyGly at pD 8.15, NaCl, and ScOMPDC in D_2O to give final concentrations of 0.74 mM h-FUMP, 12.5−82 mM guanidinium cation, and 0.08−0.12 mM ScOMPDC at $I = 0.14$. At timed intervals, during each set of experiments, 20 μL of neat deuterium labeled formic acid (DCOOD) was added to a measured aliquot that contains 0.38 or 0.75 μmol of h-FUMP + d-FUMP to quench the reaction. The enzyme was removed by ultracentrifugation using an Amicon Ultrafiltration device (10 KDa MWCO), the volume of the filtrate was adjusted to 700 μL with D_2O, and the solution was transferred to an NMR tube for analysis of the formation of d-FUMP. The enzyme-catalyzed deuterium exchange reactions were monitored for up to 2 days, during which time the activity of ScOMPDC was determined by a standard assay. In several cases, the enzyme was removed after completion of the reaction by the filtration procedures described above and the solution pD was determined. No significant loss in enzymatic activity (<5%) or decrease in solution pD (<0.1 unit) was observed during the course of these enzyme-catalyzed deuterium exchange reactions.

The ^{19}F NMR spectra were determined to give the integrated peak areas for the doublet of doublets with area (A_H) at −165.36 ppm for h-FUMP and the broad upfield-shifted apparent doublet with area (A_D) at −165.66 ppm for d-FUMP. The initial velocity (v_i, eq 1) for the enzyme-catalyzed deuterium exchange reactions of h-FUMP was determined as the slopes of the linear plots of $f_P[\textbf{FUMP}]_o$ against time over the first 5−10% reaction, where $f_P = A_D/(A_H + A_D)$ is the fraction of total **FUMP** labeled with deuterium at the C-6 position and $[\textbf{FUMP}]_o$ is the initial concentration of h-FUMP.

$$v_i = \left(\frac{d\{f_P[\textbf{FUMP}]_o\}}{dt} \right) \tag{1}$$

■ RESULTS

The decarboxylation of OMP catalyzed by the R235A mutant of ScOMPDC was monitored spectrophotometrically at wavelengths chosen to ensure that $A_i < 2.0$ for the initial absorbance of the **OMP**. Figure 2 shows the dependence of the initial velocity $v_i/[E]$ on [**OMP**] for decarboxylation reactions catalyzed by the R235A mutant of OMPDC at 25 °C, pH 7.1 (30 mM MOPS), and at different ionic strengths maintained with NaCl. Table S1 (Supporting Information) reports the
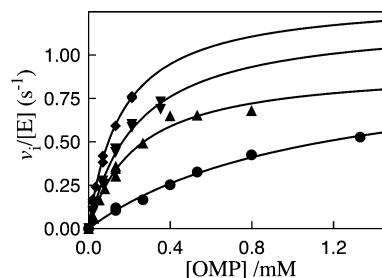

Figure 2. Michaelis−Menten plots that show the dependence of $v_i/[E]$ for decarboxylation of **OMP** catalyzed by R235A mutant ScOMPDC on the concentration of **OMP** for reactions at 25 °C, pH 7.1 (30 mM MOPS) and at different ionic strengths maintained with NaCl: ●, $I =$ 0.10; ▲, $I = 0.050$; ▼, $I = 0.035$; ◆, $I = 0.020$.

individual values of $v_i/[E]$ and the wavelengths monitored for these experiments. The solid lines for Figure 2 show the nonlinear least-squares fits of the experimental data to the Michaelis−Menten equation. The following values of k_{cat}, K_m, and k_{cat}/K_m for decarboxylation of OMP catalyzed by R235A mutant ScOMPDC were obtained from these fits, where the quoted uncertainties represent the 95% confidence interval: ●, $I = 0.10$, $k_{cat} = 1.0 \pm 0.19$ s^{-1}, $K_m = (1.1 \pm 0.36) \times 10^{-3}$ M, $k_{cat}/K_m = 910$ M^{-1} s^{-1}; ▲, $I = 0.050$, $k_{cat} = 0.93 \pm 0.11$ s^{-1}, $K_m = (0.23 \pm 0.065) \times 10^{-3}$ M, $k_{cat}/K_m = 4000$ M^{-1} s^{-1}; ▼, $I = 0.035$, $k_{cat} = 1.21 \pm 0.15$ s^{-1}, $K_m = (0.23 \pm 0.052) \times 10^{-3}$ M, $k_{cat}/K_m = 5300$ M^{-1} s^{-1}; ◆, $I = 0.020$, $k_{cat} = 1.33 \pm 0.10$ s^{-1}, $K_m = (0.16 \pm 0.022) \times 10^{-3}$ M, $k_{cat}/K_m = 8300$ M^{-1} s^{-1}.

The R235A mutant ScOMPDC-catalyzed deuterium exchange reactions of **h-FUMP** in solutions buffered by 50 mM GlyGly in D$_2$O at pD 8.15 and 25 °C were monitored by ^{19}F NMR spectroscopy at 470 MHz, as described in an earlier study of the wild-type enzyme-catalyzed deuterium exchange reactions of 1-(β-D-erythrofuranosyl) 5′-fluorouracil (**FEU**).[20] The initial reaction velocities (v_i) were determined as described in the Experimental Section. The dependence of $v_i/[E]$ on the concentration of the substrate is shown in Figure 3. These data were fit to eq 2, derived for Scheme 3, to give the values for k_{ex} and K_d reported in Table 1.

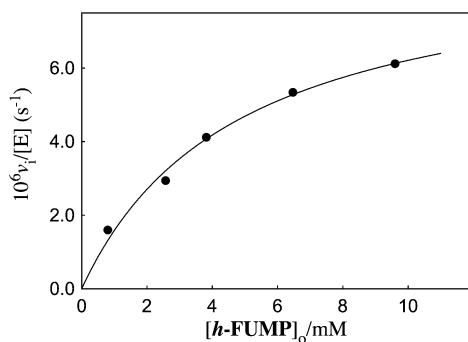$$\frac{v_i}{[E]} = \frac{k_{ex}[\textbf{h-FUMP}]_o}{[\textbf{h-FUMP}]_o + K_d} \tag{2}$$

Figure 3. Dependence of $v_i/[E]$ on the concentration of substrate **h-FUMP** for the deuterium exchange reaction catalyzed by the R235A mutant of ScOMPDC at pD 8.15 (20 mM GlyGly, 20% free base), and $I = 0.14$ (NaCl). The solid line shows the correlation of the experimental data to eq 2 derived for Scheme 3, using the values for the kinetic parameters reported in Table 1.
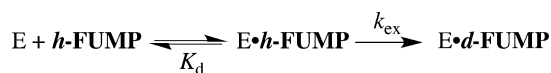
Scheme 3

$$E + \textbf{h-FUMP} \underset{K_d}{\rightleftarrows} E\cdot\textbf{h-FUMP} \xrightarrow{k_{ex}} E\cdot\textbf{d-FUMP}$$

Figure 4 shows the effect of increasing concentrations of guanidinium cation (Gua$^+$) on the relative initial velocity, $(v_i)_{obs}/(v_i)_o$, for the R235A mutant ScOMPDC-catalyzed deuterium exchange reaction of 0.74 mM **h-FUMP** at 25 °C in solutions buffered by 50 mM GlyGly at pD 8.15 and an ionic strength of 0.14 (NaCl), and the decarboxylation reaction of 5 μM **OMP** reported in an earlier study. In each case, the substrate concentration $[\textbf{h-FUMP}]_o \ll K_d = 5$ mM or $[\textbf{OMP}]_o \ll K_d = 1$ mM is far below saturation, so that in the absence of Gua$^+$ the enzyme exists mainly in the unliganded form. The data in Figure 4 show that Gua$^+$ provides quantitatively similar

activation of R235A ScOMPDC-catalyzed decarboxylation and deuterium exchange reactions. The protocol to monitor R235A mutant ScOMPDC-catalyzed deuterium exchange reactions of **FUMP** is labor intensive and consumes large amounts of enzyme. This prohibited the determination of kinetic parameters for activation of the mutant enzyme-catalyzed deuterium exchange reaction by Gua$^+$ for comparison with previously published kinetic parameters for Gua$^+$ activation of mutant enzyme-catalyzed decarboxylation of **OMP**.[27]
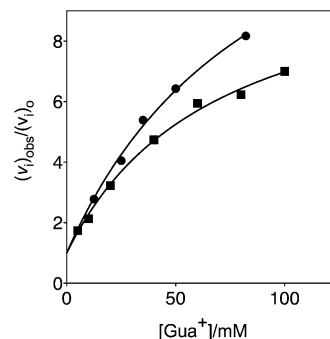

Figure 4. Dependence of $(v_i)_{obs}/(v_i)_o$ on concentration of guanidinium cation for R235A mutant ScOMPDC-catalyzed reactions, where $(v_i)_o$ is the observed initial velocity in the absence of the cation activator: ●, the deuterium exchange reaction of 0.74 mM **h-FUMP** catalyzed by the R235A mutant of ScOMPDC at pD 8.15 (20 mM GlyGly, 20% free base), 25 °C and $I = 0.14$ (NaCl); ■, the decarboxylation reaction of 5 μM **OMP** at pH 7.1 (10 mM MOPS), 25 °C and $I = 0.10$ (NaCl).[27]

The initial velocity of R235A mutant ScOMPDC-catalyzed decarboxylation of **FOMP** at 25 °C was determined for reactions at several concentrations of **FOMP** between 0.10 and 1.0 mM in solutions buffered by 10 mM MOPS at pH 7.1 and at $I = 0.10$ (NaCl). Values of k_{cat} and K_m for R235A mutant enzyme-catalyzed decarboxylation of **FOMP** were obtained from the nonlinear least-squares fits of the values of $v_i/[E]$ to the Michaelis−Menten equation (Table 1). The following parameters for ScOMPDC-catalyzed reactions, determined in earlier work at pH 7.1 and 25 °C, are reported in Table 1: k_{cat} and K_m for wild-type ScOMPDC-catalyzed decarboxylation of **OMP**[38] and **FOMP**;[39] k_{ex} and K_d for the wild-type enzyme-catalyzed deuterium exchange reaction of **h-FUMP**.[13]

Figure 5 shows the increase, at increasing concentrations of phosphite dianion, in the apparent second-order rate constant $(k_{cat}/K_m)_{obs}$ for R235A mutant ScOMPDC-catalyzed decarboxylation of **FEO** at pH 7.0 (25 mM MOPS), 25 °C, and an ionic strength of 0.14 (NaCl). A linear least-squares fit of these data to eq 3, derived for Scheme 4 ($K_d \gg [\text{HPO}_3^{2-}]$), gives the values of $(k_{cat}/K_m)_E$ and $[(k_{cat}/K_m)_{E\cdot HPi}]/K_d$ reported in Table 2. Table 2 also reports these kinetic parameters for wild-type ScOMPDC-catalyzed decarboxylation of **FEO** and for wild-type and R235A mutant ScOMPDC-catalyzed decarboxylation of **EO**, determined in earlier studies.[19,28]

$$\left(\frac{k_{cat}}{K_m}\right)_{obs} = \left(\frac{k_{cat}}{K_m}\right)_E + \left(\frac{[\text{HPO}_3^{2-}]}{K_d}\right)\left(\frac{k_{cat}}{K_m}\right)_{E\cdot HPi} \tag{3}$$

Table 1. Kinetic Parameters for the Decarboxylation and Deuterium Exchange Reactions Catalyzed by Wild-Type and R235A ScOMPDC[a]

	k_{cat} or k_{ex} (s^{-1})		K_m or K_d (M)		k_{cat}/K_m or k_{ex}/K_d (M^{-1} s^{-1})	
	wild type	R235A	wild type	R235A	wild type	R235A
OMP[b]	15	1.0	1.4×10^{-6}	1.1×10^{-3}	1.1×10^7	910
effect of mutation	15-fold decrease		790-fold increase		12000-fold decrease	
FOMP[c]	95	92	8×10^{-6}	5.8×10^{-4}	1.2×10^7	1.6×10^5
effect of mutation	no effect		73-fold increase		75-fold decrease	
h-FUMP[d]	0.044	9.3×10^{-6}	1.1×10^{-4}	5.0×10^{-3}	400	1.9×10^{-3}
effect of mutation	4700-fold decrease		45-fold increase		210000-fold decrease	

[a]Kinetic parameters k_{cat} and K_m, k_{ex} and K_d, respectively, are used for the ScOMPDC-catalyzed decarboxylation and deuterium exchange reactions. [b]At pH 7.1 (30 mM MOPS), 25 °C, and $I = 0.10$ (NaCl). Data for wild-type ScOMPDC is from ref 38. [c]At pH 7.1 (10 mM MOPS), 25 °C, and $I = 0.10$ (NaCl). Data for wild-type ScOMPDC is from ref 39. [d]At pD 8.15 (20 mM GlyGly, 20% free base), and $I = 0.14$ (NaCl). Data for wild-type ScOMPDC is from ref 13.
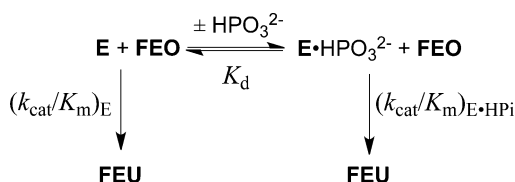
Scheme 4

$$E + FEO \underset{K_d}{\overset{\pm\ HPO_3^{2-}}{\rightleftharpoons}} E \cdot HPO_3^{2-} + FEO$$

$(k_{cat}/K_m)_E \downarrow \qquad\qquad (k_{cat}/K_m)_{E \cdot HPi} \downarrow$

$$FEU \qquad\qquad\qquad FEU$$

Table 2. Kinetic Parameters from Scheme 4 for Decarboxylation Reactions of Substrate Pieces Catalyzed by Wild-Type and R235A Mutant ScOMPDC[a]

	EO + HPO$_3^{2-}$		FEO + HPO$_3^{2-}$	
ScOMPDC	$(k_{cat}/K_m)_E$ (M^{-1} s^{-1})	$\dfrac{(k_{cat}/K_m)_{E \cdot HPi}}{K_d}$ (M^{-2} s^{-1})	$(k_{cat}/K_m)_E$ (M^{-1} s^{-1})	$\dfrac{(k_{cat}/K_m)_{E \cdot HPi}}{K_d}$ (M^{-2} s^{-1})
wild type[b]	0.026	1.2×10^4	10	4.8×10^4
R235A	0.026[c]	0.63[c]	12	250 ± 15

[a]Second-order rate constants reported in this table are reproducible to better than ±10%. [b]Data for the wild-type ScOMPDC-catalyzed reactions of EO and FEO are from refs 19 and 28, respectively. [c]Reference 19.
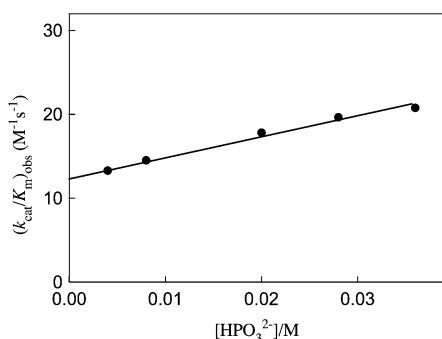

Figure 5. Dependence of observed second-order rate constant $(k_{cat}/K_m)_{obs}$ for R235A mutant of ScOMPDC-catalyzed decarboxylation of truncated substrate **FEO** on concentration of added phosphite dianion at pH 7.0, 25 °C, and $I = 0.14$ (NaCl). The solid line shows the linear correlation of the experimental data to eq 3, derived for Scheme 4, by using the values for the kinetic parameters reported in Table 2.

■ DISCUSSION

The 7-fold increase in K_m (Figure 2) for decarboxylation of **OMP** catalyzed by the R235A mutant of ScOMPDC as the ionic strength is increased from 0.020 ($K_m = 0.16 \times 10^{-3}$ M) to 0.10 ($K_m = 1.1 \times 10^{-3}$ M) shows that great care must be exercised to maintain constant ionic strength in these experiments. A similar effect of changing ionic strength on K_m has been reported for triosephosphate isomerase (TIM)-catalyzed isomerization of glyceraldehyde 3-phosphate.[40] This increase in K_m is consistent with a decrease in the activity coefficient for the substrate phosphodianion at increasing ionic strength.[41] The ScOMPDC-catalyzed deuterium exchange reactions of **h-FUMP** were carried at pD 8.15, because this is very close to the pH optimum of k_{ex}/K_d for the deuterium exchange reactions catalyzed by wild-type ScOMPDC. Similar values of $k_{cat}/K_m = 5.5 \times 10^6$ and 1.1×10^7 M^{-1} s^{-1} were determined for wild-type ScOMPDC-catalyzed decarboxylation of **OMP** at pD = 8.15 and at pH 7.1, respectively.[20]

Role of Arg235 in ScOMPDC-Catalyzed Decarboxylation and Deuterium Exchange Reactions. Table 3 summarizes the effects of the R235A mutation on the second-order rate constants k_{cat}/K_m for several ScOMPDC-catalyzed reactions and the stabilizing interaction between the side chain cation and the different reaction transition states. The essentially full ^{13}C kinetic isotope effect on k_{cat}/K_m for ScOMPDC-catalyzed decarboxylation of **OMP** is consistent with the expression of the entire side chain interaction at the rate-determining transition state.[34] However, it has been determined that the rate constant k_{-d} for the breakdown of E·**OMP** to E + **OMP** is only 4-fold larger than k_{cat} for turnover of **OMP**,[42] so that substrate binding is weakly rate determining for the second-order rate constant k_{cat}/K_m.[29,42] We calculate that $k_{cat}/K_m = 1.1 \times 10^7$ M^{-1} s^{-1} (Table 1) is 20% smaller than that for a hypothetical reaction where **OMP** binds reversibly and the chemistry is rate determining for decarboxylation. This gives an estimated interaction energy of 5.6 kcal/mol that is 0.1 kcal/mol larger than the value of 5.5 kcal/mol calculated using the observed value of $k_{cat}/K_m = 1.1 \times 10^7$ M^{-1} s^{-1} (Table 3).

The intrinsic phosphodianion binding energy may be utilized to induce electrostatic stress into the protein catalyst and/or substrate, which is relieved at the transition state for the enzyme-catalyzed decarboxylation reaction.[43−45] However, such ground state destabilization would result in equal increases in k_{cat} and K_m but should not affect the value of k_{cat}/K_m. It is therefore not relevant to our analysis of the effect of the R235A mutation on k_{cat}/K_m for the ScOMPDC-catalyzed reactions of **OMP** and **FOMP** summarized in Table 3. The utilization of

Table 3. Apparent Interaction Energies of Cationic Side Chain of Arg235 with Rate-Determining Transition States for Several ScOMPDC-Catalyzed Reactions

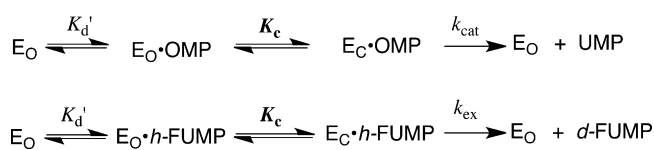| substrate	$\dfrac{(k_{cat}/K_m)_{WT}}{(k_{cat}/K_m)_{R235A}}$	interaction energy (kcal/mol)
OMP[a]	1.2×10^4	5.5^b
		5.6^c
FOMP[a]	75	2.6
h-FUMP[a]	2.1×10^5	7.2
EO[d]	1	0
FEO[d]	0.8	−0.1
HPO_3^{2-} (1 M) + **EO**[e]	1.9×10^4	5.8
HPO_3^{2-} (1 M) + **FEO**[e]	190	3.1

[a]Calculated from data in Table 1. [b]Observed stabilization of the rate-determining transition state. [c]Estimated stabilizing interaction if chemistry were fully rate determining for ScOMPDC-catalyzed decarboxylation of **OMP**. [d]Calculated from data in Table 2. [e]Calculated from the effect of the R235A mutation on $(k_{cat}/K_m)_{E \cdot HPi}/(K_d)$ (Table 2).

phosphodianion binding energy to induce electrostatic stress between protein and substrate carboxylate anions, which is relieved in the vinyl carbanion-like transition state for the enzyme-catalyzed decarboxylation reaction, would result in a smaller effect of the R235A mutation on the kinetic parameter k_{cat} for the enzyme-catalyzed deuterium exchange reaction of an unstrained Michaelis complex to **FUMP** through a vinyl carbanion-like transition state. We find, instead, that the R235A mutation results in a larger decrease in the k_{ex} for the OMPDC-catalyzed deuterium exchange reaction of **FUMP** compared with the k_{cat} for enzyme-catalyzed decarboxylation of **OMP**.

The cationic side chain of Arg235 provides no stabilization of the transition states for enzyme-catalyzed decarboxylation of the truncated substrates **EO** and **FEO** but large 5.6 and 7.2 kcal/mol stabilization, respectively, of the transition states for the decarboxylation and deuterium exchange reactions of phosphorylated substrates **OMP** and **FUMP** (Table 3). The absence of stabilizing interactions between this side chain and the decarboxylation transition state, when there is no substrate phosphodianion, shows that the large transition state stabilization observed for the OMPDC-catalyzed reactions of **OMP** and **UMP** is due entirely to stabilizing interactions expressed at the enzyme−phosphodianion ion pair (Figure 1). These interactions are not only expressed at the ground state Michaelis complex (K_m effect) because the R235A mutation results in decreases in k_{cat} and k_{ex}, respectively, for the ScOMPDC-catalyzed reactions of **OMP** and **FUMP** (Scheme 5).

We have proposed that the binding energy from the protein−phosphodianion pair is utilized to drive an enzyme conformational change that activates OMPDC for cataly-

Scheme 5

$$E_O \underset{K_d'}{\rightleftarrows} E_O \cdot OMP \underset{K_c}{\rightleftarrows} E_C \cdot OMP \xrightarrow{k_{cat}} E_O + UMP$$

$$E_O \underset{K_d'}{\rightleftarrows} E_O \cdot h\text{-FUMP} \underset{K_c}{\rightleftarrows} E_C \cdot h\text{-FUMP} \xrightarrow{k_{ex}} E_O + d\text{-FUMP}$$

sis.[19,25,28,46,47] This is shown by Scheme 5 for ScOMPDC-catalyzed reactions of **OMP** and **h-FUMP**, as the conversion of a dominant inactive open form of OMPDC (E_O) to the active closed (E_C) forms $E_C \cdot OMP$ or $E_C \cdot h\text{-FUMP}$ ($K_c \ll 1$).[22,47] The utilization of the dianion binding interactions to stabilize E_C results in enzyme activation because of the increase in the fraction of total OMPDC present as reactive E_C. The conformational change from $E_O \cdot OMP$ to $E_C \cdot OMP$ or from $E_O \cdot h\text{-FUMP}$ to $E_C \cdot h\text{-FUMP}$ includes closure of a phospho-dianion gripper loop (Pro202 to Val220) and of a hydrophobic pyrimidine umbrella (Ala151−Thr165) over O-4 and C-5 of the pyrimidine ring (Figure 6). The formation of a hydrogen
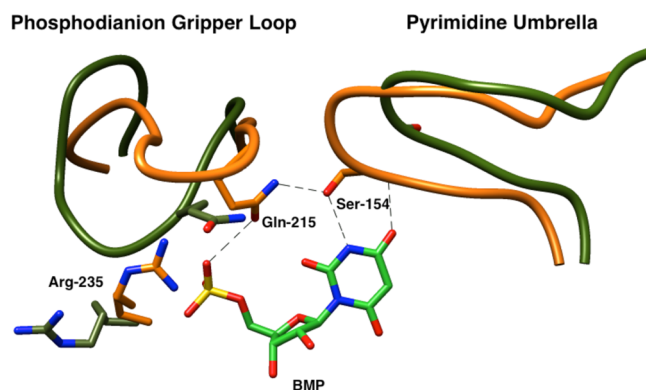

Figure 6. Image that superimposes the partial X-ray crystal structure of ScOMPDC complexed with **BMP** (PDB entry: 1DQX) over the structure for unliganded ScOMPDC (PDB entry: 1DQW). The movement of the phosphodianion gripper loop (Pro202 to Val220) toward the hydrophobic pyrimidine umbrella (Ala151−Thr165) is shown for the unliganded (orange) and liganded (olive green) enzymes. The closure of these loops is proposed to be cooperative and driven by the formation of a hydrogen bond between the side chains of Gln215 from the gripper loop and of Ser 154 from the "umbrella".

bond at E_C between the side chains of Gln 215 from the "gripper" loop and Ser154 from the "lid" shows that these structural elements act cooperatively during the enzyme conformational change.[48] The mechanism for activation of OMPDC for catalysis of decarboxylation and deuterium exchange reactions, which we propose results from this conformational change, has not been determined. A minimal mechanism would include the following: (a) the utilization of substrate binding energy for the optimal positioning of amino acid residues at the enzyme active site;[49,50] (b) the utilization of substrate binding energy to extrude solvent from the active site (this will reduce the effective dielectric constant at the active site cavity) to enhance stabilizing electrostatic interactions between the protein and transition state.[46,49,50]

Effects on k_{cat} and K_m. The ion pair between the side chain cation of Arg235 and the phosphodianion of ligands (Figure 1) appears to stabilize the enzyme−ligand complex, so that strong phosphodianion binding interactions will favor tight substrate binding. On the other hand, binding energy that is utilized to drive an initially unfavorable, but activating, protein conformational change (Scheme 5) cannot be expressed as a decrease in K_m and must instead result in an increase in k_{cat} conversion of the Michaelis complex to product.[25]

Removing the side chain cation−phosphodianion pair by the R235A mutation results in changes in both K_m or K_d for formation of the Michaelis complex to **OMP** and **h-FUMP**, respectively, and in k_{cat} or k_{ex} for conversion of the Michaelis

complex to product (Table 1). The 7.2 kcal/mol stabilizing interaction between the side chain of Arg235 and the transition state for the ScOMPDC-catalyzed deuterium exchange reaction of **h-FUMP** (Table 3) reflects a 2.2 kcal/mol stabilization of the Michaelis complex (K_d effect) and a larger 5.0 kcal/mol decrease in the barrier for conversion of the Michaelis complex to the reaction transition state (k_{ex} effect). By contrast, the smaller 5.6 kcal/mol stabilizing interaction between the side chain of Arg235 and the transition state for the decarboxylation reaction reflects a large 4.0 kcal/mol stabilization of the Michaelis complex to **OMP** (K_m effect) and only a 1.6 kcal/mol decrease in the barrier to turnover of this complex (k_{cat} effect).

$$v = \frac{\left(\frac{k_{ex}K_c}{1 + K_c}\right)[\textbf{h-FUMP}]}{\left(\frac{K_d'}{1 + K_c}\right) + [\textbf{h-FUMP}]} \tag{4}$$

$$(k_{ex})_{obs} = \left(\frac{k_{ex}K_c}{1 + K_c}\right) \tag{5}$$

$$(K_d)_{obs} = \left(\frac{K_d'}{1 + K_c}\right) \tag{6}$$

Figure 7 shows the complexes between **h-FUMP** and the open form (E_O) and the closed form (E_C) of ScOMPDC, which
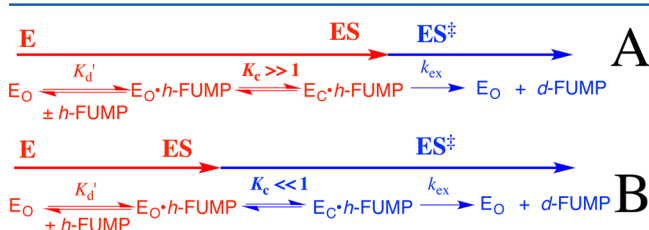

Figure 7. Diagrams that illustrate the effect of a conformational change that converts OMPDC from an inactive [nonproductive] open form to an active [productive] closed form on the kinetic parameters $(k_{ex})_{obs}$ and $(K_d)_{obs}$ for the OMPDC-catalyzed deuterium exchange reaction of **h-FUMP** to form **d-FUMP** (eqs 5 and 6). The steps leading to formation of the major Michaelis complex are shown in red, and the steps leading from this Michaelis complex to the transition state for OMPDC-catalyzed deuterium exchange are shown in blue. (A) $K_c \gg 1$. The major Michaelis complex is the productive complex $E_C \cdot$**h-FUMP** and a change in K_c affects $(K_d)_{obs}$ for substrate binding, but not $(k_{ex})_{obs}$, for turnover to form product (eq 6). (B) $K_c \ll 1$. The major Michaelis complex is the nonproductive complex $E_O \cdot$**h-FUMP**, so that the enzyme conformational change lies on the pathway from the major complex $E_O \cdot$**h-FUMP** to the reaction transition state. A change in K_c now results mainly in a change in $(k_{ex})_{obs}$ for turnover of **h-FUMP** (eq 5).

are interconverted with an equilibrium constant K_c. Equations 4−6 define the relationships between K_c, K_d', and k_{ex} from Figure 7 and the observed kinetic parameters $(k_{ex})_{obs}$ and $(K_d)_{obs}$ for the ScOMPDC-catalyzed deuterium exchange reactions of **h-FUMP**. A similar set of equations for $(k_{cat})_{obs}$ and $(K_m)_{obs}$ can be written for the ScOMPDC-catalyzed decarboxylation of **OMP**. Figure 7 shows limiting cases for the effect of a change in the protein cation−phosphodianion interaction, which affects the value of K_c, on the observed kinetic parameters. When $E_C \cdot$**h-FUMP** is the dominant complex ($K_c \gg 1$, Figure 7A), then changes in K_c will be expressed as changes in the observed substrate affinity $((K_d)_{obs},$

eq 6), and when unreactive $E_O \cdot$**h-FUMP** is the dominant complex ($K_c \ll 1$, Figure 7B), then changes in K_c will be expressed as changes in the apparent reactivity of the Michaelis complex $((k_{ex})_{obs}$, eq 5), because the enzyme conformational change is a step on the pathway from the major complex $E_O \cdot$**h-FUMP** to the reaction transition state. Mutations that result in a change from $K_c > 1$ to $K_c < 1$ will be expressed as changes in both $(K_d)_{obs}$ and $(k_{ex})_{obs}$.

OMP and **FUMP** bind to different protonated and neutral forms of OMPDC with K_d = 1.0 μM[42] and 20 μM,[13] respectively. The ligand binding is proposed to be controlled by the protonation state of the cationic side chain of Lys93.[13] Now, the effect of the R235A mutation is expressed mainly as a change in $(k_{ex})_{obs}$ for the ScOMPDC-catalyzed deuterium exchange reaction of **h-FUMP**. This is consistent with a small favorable thermodynamic driving force for the enzyme conformational change, from $E_O \cdot$**h-FUMP** to $E_C \cdot$**h-FUMP** for wild-type ScOMPDC, and a large barrier to this conformational change ($K_c \ll 1$) for the R235A mutant enzyme. The higher affinity of **OMP**, compared with that of **UMP**, for OMPDC reflects stabilizing binding interactions between the carboxylate side chain of **OMP** and the cationic side chain of Lys93.[13] We propose that these and possibly other interactions with this $-CO_2^-$ are part of an extended network of cooperative interactions that stabilize $E_C \cdot$**OMP** so that $(K_c)_{OMP} > (K_c)_{FUMP}$. This more favorable conformational change at the Michaelis complex to **OMP** compared with **h-FUMP** would result in the larger observed fractional expression of the effect of the R235A mutation on K_m (4.0/5.6 = 0.71) and a corresponding smaller observed fractional expression on k_{cat} (1.6/5.6 = 0.29) for the enzyme-catalyzed decarboxylation reaction of **OMP** compared with the fractional expression of the effect of the R235A mutation on K_d (2.2/7.2 = 0.31) and on k_{ex} (5.0/7.2 = 0.69) for the OMPDC-catalyzed deuterium exchange reaction of **h-FUMP**. The difference in the effects of the R235A mutation on the kinetic parameters for ScOMPDC-catalyzed decarboxylation of **OMP** and the deuterium exchange reaction of **FUMP** is illustrated by the two free energy profiles shown in Figure 8, and additional discussion for these differences is presented in the figure legend.

In summary, a mutation that destabilizes the closed form of wild-type OMPDC by weakening the interactions with the substrate phosphodianion will result in a decrease in substrate affinity (Figure 7A, K_d effect) up to the point where $K_c = 1$ and $(K_d)_{obs} \approx K_d'$. A further destabilization of the closed enzyme will then be expressed as an increase in the barrier for conversion of $E_O \cdot$**h-FUMP** to the rate-determining transition state (Figure 7B, k_{ex} effect). The partitioning of the overall effect on k_{cat}/K_m or k_{ex}/K_d into effects on substrate binding and catalysis depends upon the initial value of K_c for the conformational change at the Michaelis complex, and we propose that this is more favorable for the binding and reaction of **OMP** compared with **h-FUMP**.

Stabilization of Vinyl Carbanion-Like Transition States. Binding interactions between the phosphodianion and the side chain cation of Arg235 provide a strong stabilization of the vinyl carbanion-like transition states for both enzyme-catalyzed decarboxylation and deuterium exchange reactions (Table 1). Similarly, interactions between the phosphodianion and exogenous guanidinium cation provide similar activation of R235A mutant enzyme-catalyzed decarboxylation and deuterium exchange reactions (Figure 4). This result is consistent with a similar stabilization of these two vinyl
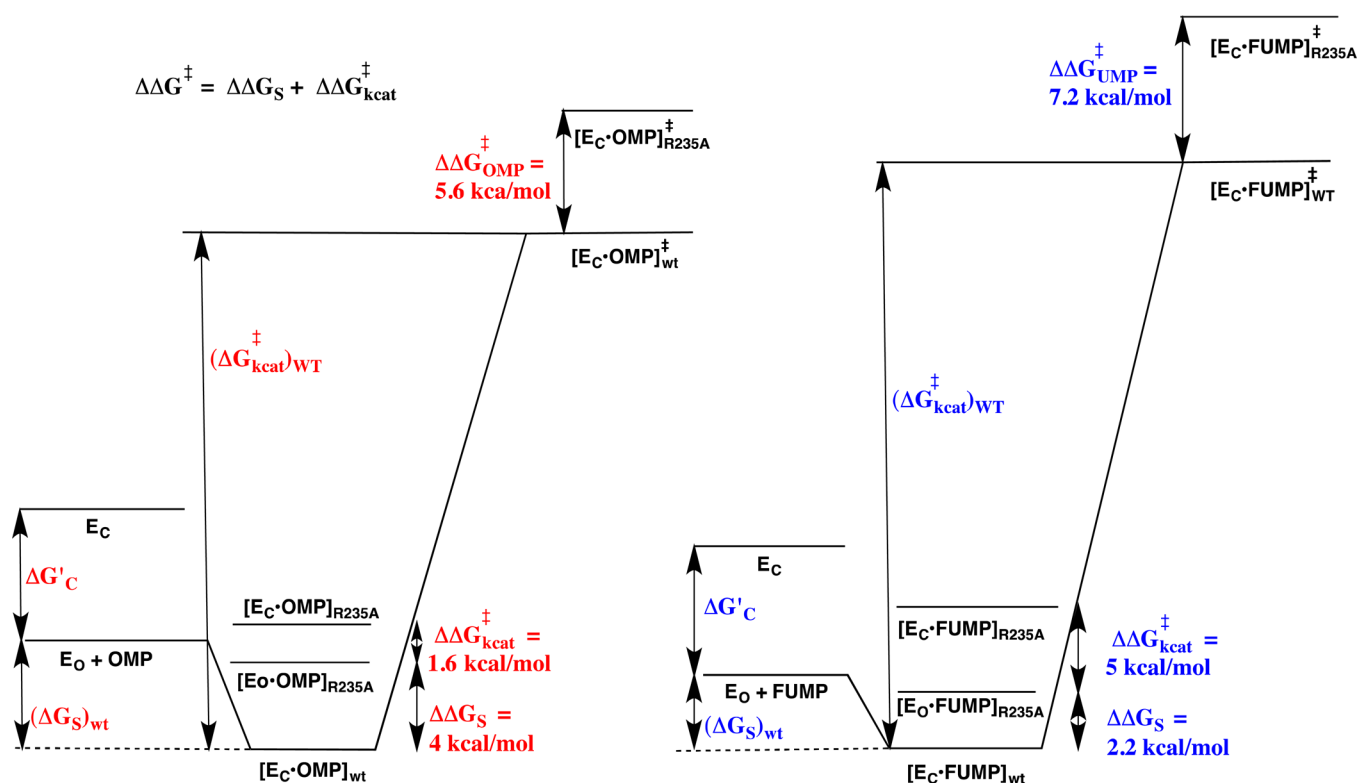
$$\Delta\Delta G^{\ddagger} = \Delta\Delta G_{S} + \Delta\Delta G^{\ddagger}_{kcat}$$

Figure 8. Free energy reaction profiles that illustrate different effects of R235A mutation on kinetic parameters. Profiles shown are for *Sc*OMPDC-catalyzed decarboxylation of **OMP** to form **UMP** (profile on left) and the deuterium exchange reaction of *h*-**FUMP** to form *d*-**FUMP** (profile on right). The binding energy of R235A and other residues in the phosphodianion gripper loop is utilized to drive the conversion of open enzyme E_O to closed enzyme E_C. This binding energy is partly expressed at the Michaelis complex when loop closure at the Michaelis complex is thermodynamically favorable ($K_c > 1$, eqs 4−6). The substrate binding energy $(\Delta G_S)_{wt}$ of **OMP** is greater than that for **FUMP**, and we propose that this reflects the utilization of the binding interactions with the $-CO_2^-$ group of OMP to drive the conversion of E_O to E_C ($\Delta G'_c$). The overall effect of the R235A mutation on the barrier for the deuterium exchange ($\Delta\Delta G^{\ddagger}_{UMP}$ = 7.2 kcal/mol) is larger than that for the decarboxylation reaction ($\Delta\Delta G^{\ddagger}_{OMP}$ = 5.6 kcal/mol). The R235A mutation results mainly in a decrease in ΔG_S for the decarboxylation reaction ($\Delta\Delta G_S$ = 4 kcal/mol). We propose that the Michaelis complex between **OMP** and the R235A mutant enzyme exists mainly in the nonproductive open form ($[E_O\cdot OMP]_{R235A}$), because there is insufficient binding energy at this Michaelis complex enzyme to drive the enzyme conformational change ($K_c < 1$, eqs 4−6). The effect of the R235A mutation on k_{cat} ($\Delta\Delta G^{\ddagger}_{kcat}$ = 1.6 kcal/mol) is shown as the 1.6 kcal/mol barrier for conversion of $[E_O\cdot OMP]_{R235A}$ to the productive complex ($[E_C\cdot OMP]_{R235A}$). The smaller binding energy from **FUMP** compared with **OMP** available to drive the enzyme conformational change ($(K_c)_{FUMP} < (K_c)_{OMP}$, eqs 4−6) results in the smaller the effect of the R235A mutation on ΔG_S ($\Delta\Delta G_S$ = 2.2 kcal/mol) and a large 5 kcal/mol barrier to conversion of nonproductive $[E_O\cdot FUMP]_{R235A}$ to productive ($[E_C\cdot FUMP]_{R235A}$ that is added to the barrier for conversion of $[E_O\cdot FUMP]_{R235A}$ to product ($\Delta\Delta G^{\ddagger}_{kcat}$ = 5 kcal/mol).

carbanion-like transition states by interaction with Gua[+].[13,14,20] This limited set of data shows that the deuterium exchange and decarboxylation reactions catalyzed by this mutant OMPDC are activated to a similar degree by Gua[+], and that the side chain shows similar effective molarities in the two reactions.[27]

The apparent interaction of the cationic side chain of Arg235 with the transition state for the *Sc*OMPDC-catalyzed deuterium exchange reaction (7.2 kcal/mol) is larger than the interaction with the transition state for the enzyme-catalyzed decarboxylation reaction (5.6 kcal/mol), but the 5.6 kcal/mol interaction energy is 50% of the total 11.2 kcal/mol contribution of the phosphodianion binding energy to the stabilization of the decarboxylation transition state,[18] whereas the 7.2 kcal/mol interaction is a larger 78% of the total 9.2 kcal/mol contribution of the phosphodianion binding energy to the stabilization of the exchange transition state.[20]

We speculate that the 2 kcal/mol larger phosphodianion binding energy utilized to stabilize the transition state for OMPDC-catalyzed decarboxylation of **OMP** compared with the deuterium exchange reaction of *h*-**FUMP** reflects the tighter fit of **OMP** at the enzyme active site. This minimizes the

entropic cost to formation of a network of hydrogen bonding and ionic interactions with the substrate phosphodianion.[51,52] We propose that there is a related greater cooperativity for **FUMP** compared with **OMP** in the expression of the phosphodianion binding interactions with the amino acid side chains of Gln215, Tyr217, and Arg235 (Figure 1) and that the large 7.2 kcal/mol effect of the R235A mutation on the stability of the transition state for the deuterium exchange reaction of *h*-**FUMP** reflects not only the loss of the interactions with the excised side chain (≈5.6 kcal/mol determined for the reaction of **OMP**) but also a ca. 1.6 kcal/mol weakening of interactions between the phosphodianion and the side chains of the remaining gripper residues Gln215 and Tyr217 (Figure 1).[53] Once again, we propose that the phosphodianion binding interactions are more fully maintained at the transition state for the R235A mutant *Sc*OMPDC-catalyzed decarboxylation, compared with the deuterium exchange reaction, because the interactions between OMPDC and the pyrimidine carboxylate have the effect of reducing the entropy of the bound substrate by "locking" the ligand into a rigid reactive conformation.[52]

***Sc*OMPDC-Catalyzed Decarboxylation of FOMP and FEO.** The cationic side chain of Arg235 provides similar 5.6 and 5.8 kcal/mol stabilization of the transition states for the *Sc*OMPDC-catalyzed reactions of **OMP** and the substrate pieces **EO** + HPO_3^{2-}, respectively, and smaller but likewise similar, 2.6 and 3.1 kcal/mol stabilization of the transition states for the enzyme-catalyzed reactions of **FOMP** and the substrate pieces **FEO** + HPO_3^{2-} (Table 3). The similar interaction of this side chain with the transition states for the reactions of the whole substrates **OMP** or **FOMP** and the corresponding substrate pieces **EO** + HPO_3^{2-} or **FEO** + HPO_3^{2-} is consistent with the conclusion that the transition states for reactions of related whole substrates and substrate pieces show essentially the same interaction with the protein catalyst.[18−20,48] The main effect of this covalent attachment is to reduce the entropic barrier for the unimolecular reaction of the whole substrate, compared with the bimolecular reaction of the corresponding pieces.[51,54]

The difference in the stabilization of the transition states for *Sc*OMPDC-catalyzed reactions of **FOMP** or **FEO** + HPO_3^{2-} compared with **OMP** or **EO** + HPO_3^{2-} by interaction with the cationic side chain of Arg235 reflects the different rate determining steps for the wild-type enzyme-catalyzed reactions of the two types of substrates.[28,29,34] The values of the kinetic parameters k_{cat}/K_m (Table 1) or $[(k_{cat}/K_m)_{E\cdot Pi}]/K_d]$ (Table 2) for the wild-type *Sc*OMPDC-catalyzed reactions of **OMP** or **EO** + HPO_3^{2-}, respectively, are limited by the rate of the chemical decarboxylation step, whereas values for the wild-type enzyme-catalyzed reactions of **FOMP** or **FEO** + HPO_3^{2-} are limited by rate constant for formation of the Michaelis complex to substrate.[28,29,34] The effect of the loss of the side chain interaction at the R235A mutant enzyme is essentially entirely expressed as the change in the values of the kinetic parameters for the wild-type *Sc*OMPDC-catalyzed reactions of substrates **OMP** or **EO** + HPO_3^{2-}, for which the chemical step is rate determining. By comparison, the effect of the R235A mutation should not result in a decrease in k_{cat}/K_m or $[(k_{cat}/K_m)_{E\cdot Pi}]/K_d]$ for the reactions of **FOMP** or **FEO** + HPO_3^{2-}, until there is a change in the rate-determining step. Our results show that this change in rate determining step only occurs after there is a ca. 3 kcal/mol increase in the barrier to the decarboxylation of enzyme-bound **FOMP** or **FEO** + HPO_3^{2}.

Summary. We have rationalized these data by a model in which the following apply: (1) The Michaelis complex between **FUMP** and R235A mutant OMPDC exists mainly in the open conformation (Figure 7B), so that the interactions with the cationic side chain of R235 at wild-type OMPDC result mainly in an increase in k_{ex} for the deuterium exchange reaction (Figure 8). (2) The stabilizing interactions between OMPDC and the $-CO_2^-$ group of **OMP** result in a shift in this conformational equilibrium to the closed form of OMPDC, so that the interactions with the cationic side chain of R235 at wild-type OMPDC now result mainly in a decrease in K_m for decarboxylation (Figure 8). (3) The stabilizing interactions between OMPDC and the $-CO_2^-$ group of **OMP** are utilized to immobilize the substrate in *Sc*OMPDC: the removal of the $-CO_2^-$ group results in a greater conformational flexibility of enzyme bound **FUMP**, a larger requirement for the utilization of the phosphodianion binding interactions to immobilize this substrate with the result that a smaller fraction of the total dianion binding energy is available to stabilize the transition state for the *Sc*OMPDC-catalyzed deuterium exchange reaction

of **FUMP** compared with the OMPDC-catalyzed decarboxylation reaction.[52]

There are interesting differences in the mechanisms for the utilization of dianion binding interactions in the activation of triosephosphate isomerase for catalysis of the truncated substrate glycolaldehyde (GA, Scheme 6) and of OMPDC

Scheme 6

h-**GA** d-**GA**
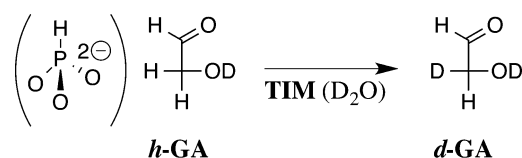
for catalysis of the decarboxylation and deuterium exchange reactions of **EO** and **FEU**, respectively (Scheme 2).[18,20,22] The binding loci for the small carbon acid GA and for HPO_3^{2-} are overlapping.[55,56] The sites behave independently to the extent that some structural mutations, which have little effect on enzyme activation by phosphite dianion, result in a decrease in the enzyme reactivity toward deprotonation of glycolaldehyde.[57] Binding of dianion activators to TIM triggers movement of active site loops 6 and loop 7. This places the active site base from Glu167 in a reactive conformation and swings the side chain of Ile172 toward the catalytic base,[55,56] with the effect of shielding the substrate and the catalytic carboxylate from interaction with bulk solvent.[55] The results of studies on the effect of the I172A mutation on the kinetic parameters for the TIM-catalyzed reactions of GA and HPO_3^{2-} provide strong evidence for the conclusion that interactions between the hydrophobic side chain of I172 and the catalytic carboxylate from Glu167 activate TIM for catalysis of deprotonation of carbon by enhancing the basicity of this carboxylate ion.[58−60]

By comparison to TIM, the binding loci for **EO** and HPO_3^{2-} are well separated at the active site of OMPDC. Binding of the dianion activator also triggers large movement of a phosphodianion gripper loop, but this loop appears too remote from the pyrimidine binding site to result in a large activation of OMPDC for catalysis of decarboxylation of **EO** (Figures 1 and 6). The results reported in this paper provide support for the conclusion that binding of the dianion activator triggers a much more extensive cooperative conformational change, which includes not only movement of the phosphodianion gripper loop but also the enzyme-activating closure of the pyrimidine umbrella. The dense network of hydrogen bonds that involve Ser154, from the pyrimidine umbrella, and Gln215, from the gripper loop should promote cooperative closure of these structural elements.[48]

■ ASSOCIATED CONTENT

Ⓢ Supporting Information

Table S1: UV wavelengths monitored in determining initial velocity data reported in Figure 2 for R235A *Sc*OMPDC-catalyzed decarboxylation of **OMP** at different ionic strengths. This material is available free of charge via the Internet at http://pubs.acs.org.

■ AUTHOR INFORMATION

Corresponding Author

*J. P. Richard. Tel: (716) 645-4232. Fax: (716) 645-6963. E-mail: jrichard@buffalo.edu.

■ ABBREVIATIONS

ScOMPDC, orotidine 5′-monophosphate decarboxylase from *S. cerevisiae*; PRPP synthase, phosphoribosylpyrophosphate synthase; ORTase, orotate phosphoribosyl transferase; TIM, triosephosphate isomerase; OMP, orotidine 5′-monophosphate; UMP, uridine 5′-monophosphate; FOMP, 5-fluoroorotidine 5′-monophosphate; FUMP, 5-fluorouridine 5′-monophosphate; *h*-FUMP, FUMP labeled with hydrogen at C-6; *d*-FUMP, FUMP labeled with deuterium at C-6; BMP, 6-hydroxyuridine 5′-monophosphate; EO, 1-(β-D-erythrofuranosyl)orotic acid; EU, 1-(β-D-erythrofuranosyl)uracil; FEO, 1-(β-D-erythrofuranosyl)-5-fluoroorotic acid; FEU, 1-(β-D-erythrofuranosyl)-5-fluorouracil; Gua$^+$, guanidinium cation; GA, glycolaldehyde; MOPS, 3-(*N*-morpholino)propanesulfonic acid; NMR, nuclear magnetic resonance

■ REFERENCES

(1) Radzicka, A., and Wolfenden, R. (1995) A proficient enzyme. *Science 267*, 90−93.

(2) Miller, B. G., Hassell, A. M., Wolfenden, R., Milburn, M. V., and Short, S. A. (2000) Anatomy of a proficient enzyme: the structure of orotidine 5′-monophosphate decarboxylase in the presence and absence of a potential transition state analog. *Proc. Natl. Acad. Sci. U. S. A. 97*, 2011−2016.

(3) Sievers, A., and Wolfenden, R. (2002) Equilibrium of Formation of the 6-Carbanion of UMP, a Potential Intermediate in the Action of OMP Decarboxylase. *J. Am. Chem. Soc. 124*, 13986−13987.

(4) Wong, F. M., Capule, C. C., and Wu, W. (2006) Stability of the 6-Carbanion of Uracil Analogues: Mechanistic Implications for Model Reactions of Orotidine-5′-Monophosphate Decarboxylase. *Org. Lett. 8*, 6019−6022.

(5) Levine, H. L., Brody, R. S., and Westheimer, F. H. (1980) Inhibition of orotidine-5′-phosphate decarboxylase by 1-(5′-phospho-β-D-ribofuranosyl)barbituric acid, 6-azauridine 5′-phosphate, and uridine 5′-phosphate. *Biochemistry 19*, 4993−4999.

(6) Houk, K. N., Lee, J. K., Tantillo, D. J., Bahmanyar, S., and Hietbrink, B. N. (2001) Crystal structures of orotidine monophosphate decarboxylase: does the structure reveal the mechanism of nature's most proficient enzyme? *ChemBioChem 2*, 113−118.

(7) Lee, T.-S., Chong, L. T., Chodera, J. D., and Kollman, P. A. (2001) An alternative explanation for the catalytic proficiency of orotidine 5′-phosphate decarboxylase. *J. Am. Chem. Soc. 123*, 12837−12848.

(8) Silverman, R. B., and Groziak, M. P. (1982) Model chemistry for a covalent mechanism of action of orotidine 5′-phosphate decarboxylase. *J. Am. Chem. Soc. 104*, 6434−6439.

(9) Beak, P., and Siegel, B. (1976) Mechanism of decarboxylation of 1,3-dimethylorotic acid. A model for orotidine 5′-phosphate decarboxylase. *J. Am. Chem. Soc. 98*, 3601−3606.

(10) Shostak, K., and Jones, M. E. (1992) Orotidylate decarboxylase: insights into the catalytic mechanism from substrate specificity studies. *Biochemistry 31*, 12155−12161.

(11) Appleby, T. C., Kinsland, C., Begley, T. P., and Ealick, S. E. (2000) The crystal structure and mechanism of orotidine 5′-monophosphate decarboxylase. *Proc. Natl. Acad. Sci. U. S. A. 97*, 2005−2010.

(12) Lee, J. K., and Houk, K. N. (1997) A proficient enzyme revisited: the predicted mechanism for orotidine monophosphate decarboxylase. *Science 276*, 942−945.

(13) Tsang, W.-Y., Wood, B. M., Wong, F. M., Wu, W., Gerlt, J. A., Amyes, T. L., and Richard, J. P. (2012) Proton Transfer from C-6 of Uridine 5′-Monophosphate Catalyzed by Orotidine 5′-Monophosphate Decarboxylase: Formation and Stability of a Vinyl Carbanion Intermediate and the Effect of a 5-Fluoro Substituent. *J. Am. Chem. Soc. 134*, 14580−14594.

(14) Amyes, T. L., Wood, B. M., Chan, K., Gerlt, J. A., and Richard, J. P. (2008) Formation and Stability of a Vinyl Carbanion at the Active Site of Orotidine 5′-Monophosphate Decarboxylase: pK_a of the C-6 Proton of Enzyme-Bound UMP. *J. Am. Chem. Soc. 130*, 1574−1575.

(15) Chan, K. K., Wood, B. M., Fedorov, A. A., Fedorov, E. V., Imker, H. J., Amyes, T. L., Richard, J. P., Almo, S. C., and Gerlt, J. A. (2009) Mechanism of the Orotidine 5′-Monophosphate Decarboxylase-Catalyzed Reaction: Evidence for Substrate Destabilization. *Biochemistry 48*, 5518−5531.

(16) Toth, K., Amyes, T. L., Wood, B. M., Chan, K., Gerlt, J. A., and Richard, J. P. (2010) Product Deuterium Isotope Effects for Orotidine 5′-Monophosphate Decarboxylase: Effect of Changing Substrate and Enzyme Structure on the Partitioning of the Vinyl Carbanion Reaction Intermediate. *J. Am. Chem. Soc. 132*, 7018−7024.

(17) Toth, K., Amyes, T. L., Wood, B. M., Chan, K., Gerlt, J. A., and Richard, J. P. (2007) Product Deuterium Isotope Effect for Orotidine 5′-Monophosphate Decarboxylase: Evidence for the Existence of a Short-Lived Carbanion Intermediate. *J. Am. Chem. Soc. 129*, 12946−12947.

(18) Amyes, T. L., Richard, J. P., and Tait, J. J. (2005) Activation of orotidine 5′-monophosphate decarboxylase by phosphite dianion: The whole substrate is the sum of two parts. *J. Am. Chem. Soc. 127*, 15708−15709.

(19) Amyes, T. L., Ming, S. A., Goldman, L. M., Wood, B. M., Desai, B. J., Gerlt, J. A., and Richard, J. P. (2012) Orotidine 5′-monophosphate decarboxylase: Transition state stabilization from remote protein-phosphodianion interactions. *Biochemistry 51*, 4630−4632.

(20) Goryanova, B., Amyes, T. L., Gerlt, J. A., and Richard, J. P. (2011) OMP Decarboxylase: Phosphodianion Binding Energy Is Used To Stabilize a Vinyl Carbanion Intermediate. *J. Am. Chem. Soc. 133*, 6545−6548.

(21) Tsang, W.-Y., Amyes, T. L., and Richard, J. P. (2008) A Substrate in Pieces: Allosteric Activation of Glycerol 3-Phosphate Dehydrogenase (NAD$^+$) by Phosphite Dianion. *Biochemistry 47*, 4575−4582.

(22) Amyes, T. L., and Richard, J. P. (2007) Enzymatic catalysis of proton transfer at carbon: activation of triosephosphate isomerase by phosphite dianion. *Biochemistry 46*, 5841−5854.

(23) Amyes, T. L., O'Donoghue, A. C., and Richard, J. P. (2001) Contribution of phosphate intrinsic binding energy to the enzymatic rate acceleration for triosephosphate isomerase. *J. Am. Chem. Soc. 123*, 11325−11326.

(24) Richard, J. P. (2012) A Paradigm for Enzyme-Catalyzed Proton Transfer at Carbon: Triosephosphate Isomerase. *Biochemistry 51*, 2652−2661.

(25) Amyes, T. L., and Richard, J. P. (2013) Specificity in Transition State Binding: The Pauling Model Revisited. *Biochemistry 52*, 2021−2035.

(26) Miller, B. G., Snider, M. J., Short, S. A., and Wolfenden, R. (2000) Contribution of Enzyme-Phosphoribosyl Contacts to Catalysis by Orotidine 5′-Phosphate Decarboxylase. *Biochemistry 39*, 8113−8118.

(27) Barnett, S. A., Amyes, T. L., McKay Wood, B., Gerlt, J. A., and Richard, J. P. (2010) Activation of R235A Mutant Orotidine 5′-Monophosphate Decarboxylase by the Guanidinium Cation: Effective Molarity of the Cationic Side Chain of Arg-235. *Biochemistry 49*, 824−826.

(28) Goryanova, B., Spong, K., Amyes, T. L., and Richard, J. P. (2013) Catalysis by Orotidine 5′-Monophosphate Decarboxylase: Effect of 5-Fluoro and 4′-Substituents on the Decarboxylation of Two-Part Substrates. *Biochemistry 52*, 537−546.

(29) Wood, B. M., Chan, K. K., Amyes, T. L., Richard, J. P., and Gerlt, J. A. (2009) Mechanism of the Orotidine 5′-Monophosphate Decarboxylase-Catalyzed Reaction: Effect of Solvent Viscosity on Kinetic Constants. *Biochemistry 48*, 5510−5517.

(30) Bhatia, M. B., Vinitsky, A., and Grubmeyer, C. (1990) Kinetic Mechanism of Orotate Phosphoribosyltransferase from *Salmonella typhimurium. Biochemistry 29*, 10480−10487.

(31) Hove-Jensen, B. (1985) Cloning and characterization of the *prs* gene encoding phosphoribosylpyrophosphate synthetase of *Escherichia coli. Mol. Gen. Genet. 201*, 269−276.

(32) Tolbert, T. J., and Williamson, J. R. (1996) Preparation of specifically deuterated RNA for NMR studies using a combination of chemical and enzymatic synthesis. *J. Am. Chem. Soc. 118*, 7929−7940.

(33) Bower, S. G., Harlow, K. W., Switzer, R. L., and Hove-Jensen, B. (1989) Characterization of the *Escherichia coli prsA1*-encoded Mutant Phosphoribosylpyrophosphate Synthetase Identifies a Divalent Cation-Nucleotide Binding Site. *J. Biol. Chem. 264*, 10287−10291.

(34) Van Vleet, J. L., Reinhardt, L. A., Miller, B. G., Sievers, A., and Cleland, W. W. (2008) Carbon isotope effect study on orotidine 5′-monophosphate decarboxylase: support for an anionic intermediate. *Biochemistry 47*, 798−803.

(35) Gross, A., Abril, O., Lewis, J. M., Geresh, S., and Whitesides, G. M. (2013) Practical synthesis of 5-phospho-D-ribosyl α-1-pyrophosphate (PRPP): enzymatic routes from ribose 5-phosphate or ribose. *J. Am. Chem. Soc. 105*, 7428−7435.

(36) Glasoe, P. K., and Long, F. A. (1960) Use of glass electrodes to measure acidities in deuterium oxide. *J. Phys. Chem. 64*, 188−190.

(37) Gasteiger, E., Gattiker, A., Hoogland, C., Ivanyi, I., Appel, R. D., and Bairoch, A. (2003) ExPASy: The proteomics server for in-depth protein knowledge and analysis. *Nucleic Acids Res. 31*, 3784−3788.

(38) Toth, K., Amyes, T. L., Wood, B. M., Chan, K. K., Gerlt, J. A., and Richard, J. P. (2009) An Examination of the Relationship between Active Site Loop Size and Thermodynamic Activation Parameters for Orotidine 5′-Monophosphate Decarboxylase from Mesophilic and Thermophilic Organisms. *Biochemistry 48*, 8006−8013.

(39) Barnett, S. A. (2009) Studies on the Mechanism of Action of Orotidine 5′-Monophosphate Decarboxylase, *Ph.D. Thesis*, University at Buffalo, Buffalo, NY.

(40) Hartman, F., Lamuraglia, G., Tomozawa, Y., and Wolfenden, R. (1975) Influence of pH on the interaction of inhibitors with triosephosphate isomerase and determination of the pK_a of the active-site carboxyl group. *Biochemistry 14*, 5274−5279.

(41) Nolte, H.-J., Rosenberry, T. L., and Neumann, E. (1980) Effective charge on acetylcholinesterase active sites determined from the ionic strength dependence of association rate constants with cationic ligands. *Biochemistry 19*, 3705−3711.

(42) Porter, D. J. T., and Short, S. A. (2000) Yeast Orotidine-5′-Phosphate Decarboxylase: Steady-State and Pre-Steady-State Analysis of the Kinetic Mechanism of Substrate Decarboxylation. *Biochemistry 39*, 11788−11800.

(43) Gao, J., Byun, K. L., and Kluger, R. (2004) Catalysis by enzyme conformational change. *Top. Curr. Chem. 238*, 113−136.

(44) Gao, J. (2003) Catalysis by enzyme conformational change as illustrated by orotidine 5'-monophosphate decarboxylase. *Curr. Opin. Struct. Biol. 13*, 184−192.

(45) Wu, N., Mo, Y., Gao, J., and Pai, E. F. (2000) Electrostatic stress in catalysis: structure and mechanism of the enzyme orotidine monophosphate decarboxylase. *Proc. Natl. Acad. Sci. U. S. A. 97*, 2017−2022.

(46) Malabanan, M. M., Amyes, T. L., and Richard, J. P. (2010) A role for flexible loops in enzyme catalysis. *Curr. Opin. Struct. Biol. 20*, 702−710.

(47) Go, M. K., Amyes, T. L., and Richard, J. P. (2009) Hydron Transfer Catalyzed by Triosephosphate Isomerase. Products of the Direct and Phosphite-Activated Isomerization of [1-^{13}C]-Glycolaldehyde in D$_2$O. *Biochemistry 48*, 5769−5778.

(48) Barnett, S. A., Amyes, T. L., Wood, B. M., Gerlt, J. A., and Richard, J. P. (2008) Dissecting the Total Transition State Stabilization Provided by Amino Acid Side Chains at Orotidine 5′-Monophosphate Decarboxylase: A Two-Part Substrate Approach. *Biochemistry 47*, 7785−7787.

(49) Warshel, A. (1998) Electrostatic Origin of the Catalytic Power of Enzymes and the Role of Preorganized Active Sites. *J. Biol. Chem. 273*, 27035−27038.

(50) Cannon, W. R., and Benkovic, S. J. (1998) Solvation, Reorganization Energy, and Biological Catalysis. *J. Biol. Chem. 273*, 26257−26260.

(51) Jencks, W. P. (1981) On the attribution and additivity of binding energies. *Proc. Natl. Acad. Sci. U. S. A. 78*, 4046−4050.

(52) Adams, H., Chekmeneva, E., Hunter, C. A., Misuraca, M. C., Navarro, C., and Turega, S. M. (2013) Quantification of the Effect of Conformational Restriction on Supramolecular Effective Molarities. *J. Am. Chem. Soc. 135*, 1853−1863.

(53) Horovitz, A., and Fersht, A. R. (1990) Strategy for analyzing the cooperativity of intramolecular interactions in peptides and proteins. *J. Mol. Biol. 214*, 613−617.

(54) Page, M. I., and Jencks, W. P. (1971) Entropic contributions to rate accelerations in enzymic and intramolecular reactions and the chelate effect. *Proc. Nat. Acad. Sci. U. S. A. 68*, 1678−1683.

(55) Kursula, I., and Wierenga, R. K. (2003) Crystal structure of triosephosphate isomerase complexed with 2-phosphoglycolate at 0.83-Å resolution. *J. Biol. Chem. 278*, 9544−9551.

(56) Jogl, G., Rozovsky, S., McDermott, A. E., and Tong, L. (2003) Optimal alignment for enzymatic proton transfer: structure of the Michaelis complex of triosephosphate isomerase at 1.2-Å resolution. *Proc. Natl. Acad. Sci. U. S. A. 100*, 50−55.

(57) Zhai, X., Amyes, T. L., Wierenga, R. K., Loria, J. P., and Richard, J. P. (2013) Structural Mutations That Probe the Interactions between the Catalytic and Dianion Activation Sites of Triosephosphate Isomerase. *Biochemistry 52*, 5928−5940.

(58) Malabanan, M. M., Nitsch-Velasquez, L., Amyes, T. L., and Richard, J. P. (2013) Magnitude and origin of the enhanced basicity of the catalytic glutamate of triosephosphate isomerase. *J. Am. Chem. Soc. 135*, 5978−5981.

(59) Malabanan, M. M., Koudelka, A. P., Amyes, T. L., and Richard, J. P. (2012) Mechanism for Activation of Triosephosphate Isomerase by Phosphite Dianion: The Role of a Hydrophobic Clamp. *J. Am. Chem. Soc. 134*, 10286−10298.

(60) Richard, J. P. (1998) The Enhancement of Enzymic Rate Accelerations by Brønsted Acid-Base Catalysis. *Biochemistry 37*, 4305−4309.